Solid Freeform Fabrication 2017: Proceedings of the 28th Annual International Solid Freeform Fabrication Symposium – An Additive Manufacturing Conference
Reviewed Paper

DIGITAL LIGHT PROCESSING (DLP): ANISOTROPIC TENSILE CONSIDERATIONS

E. Aznarte, C. Ayranci, and A.J. Qureshi

Department of Mechanical Engineering, University of Alberta, 10-203 DICE, 9211-116 Street NW, Edmonton, AB, Canada

Abstract

Digital light processing (DLP) 3D printing is an additive manufacturing (AM) process used to produce layered parts via photopolymerization. Anisotropy is a common characteristic of parts produced by DLP. Furthermore, printing conditions affect widely the resulting mechanical properties. This paper shows the effect of three printing factors on the final mechanical properties of specimens manufactured using DLP 3D printing. A series of ISO compliant tensile test specimens were designed, printed and tested. The properties analyzed were the elastic modulus, ultimate tensile strength, ultimate strain and printing time. Preliminary findings on design guidelines for Vat Photopolymerization processes are presented in addition to the economic effect of the studied parameters in terms of the total printing time.

Keywords: 3D Printing, Additive Manufacturing, Mechanical Characterization, Digital Light Processing (DLP), Vat-Photopolymerization, Stereolithography.

1. Introduction

Additive Manufacturing (AM) is the manufacturing process by which Three Dimensional (3D) parts are produced using an additive approach. Rapid prototyping was the first technology that allowed layer by layer material deposition using Computer Aided Design (CAD) (Wong and Hernandez, 2012). Stereolithography was the most popular rapid prototyping technique during the decade of 1990. It was invented in 1982 and patented in 1986 (Hull, 1986) by Charles Hull. This system builds a solid piece from a CAD model by sketching the cross section of the product with a laser beam that cures liquid photopolymer simultaneously (Comerford, 1993).

Vat Photopolymerization is a form of AM. It uses a liquid bath of a polymeric photosensitive resin that is cured layer by layer through precise control and projection of a light source. The general composition of the resin is formed of a monomer material, a photoinitiator and an absorber (Gong et al., 2015). Photopolymerization is the process of linking monomers into polymers initiated by radiation exposure. This process can be divided in three steps: initiation, propagation and termination (Fuh et al., 1999). Said radiation, due to the exothermic nature of the process, can be a low-power UV laser or light source (Fuh et al., 1999).

Parts manufactured by Vat Photopolymerization have varying mechanical properties depending upon the choice of parameters during the manufacturing. These properties depend mostly on the curing of the resin, which is affected by the power of the light source, the wavelength, the speed of construction, the resin composition and other factors (Salmoria et al., 2005). For example, a specimen subjected to a low exposure time and radiant power will be

under-cured; consequently, it would potentially have sub-par mechanical properties compared to a fully-cured specimen.

Additive manufacturing differs from classical manufacturing processes in several aspects. Due to the layer by layer technique it ends up creating a material orthotropic in nature. The AM process is usually fully digital, meaning that manufacturing process characteristics should be considered in the design stage, making the expertise of the designer a factor. The effect of the design decisions, such as part orientation or location on the base can affect the quality and properties of the part. Conventional design strategies are not sufficient to control the final properties of these parts. Consequently, with this study, we aim to achieve an early stage design method to understand and optimize the effects of printing parameters on elastic and mechanical properties of printed parts.

In this work, we are reporting our findings on the effect of three chosen parameters on the final properties of printed specimens subjected to a tensile test. The variations between specimens will be analyzed and related to one or another parameter or the combination of them. Finally, the relationship between time and mechanical properties will be discussed, including the direct relation between time and cost. This work and the ongoing studies are crucial in establishing design curves for AM based materials represented in material selection charts.

2. State of the Art

Certain combinations of printing parameters have been demonstrated to significantly improve elastic and mechanical properties of printed parts (Fatimatuzahraa et al., 2011). Unlike the bulk produced or processed conventional engineering materials, such as metals, or some polymers, the parts manufactured using AM processes demonstrate microstructural anisotropy. The said behavior mostly originates from the layer by layer and sometimes directional nature of the production of the structure (Carroll et al., 2015).

If the parts produced with AM are used without complete and fundamental understanding of this anisotropy, inconsistencies in properties can be observed (Santos et al., 2013). This, in return, will pose further challenges in design and simulation of AM parts with finite element analysis methods. Finally, another factor that may interfere with the mechanical properties is the scale at which each part is printed. When testing similar parts produced by FDM processes with infills below 100% at different scales, the scalability of mechanical properties such as Elastic modulus (E), or Ultimate Tensile Strength (UTS), difference is not proportional to the scale of the piece(Mahmood et al., 2017; Qureshi et al., 2015).

Extensive research literature is available on FDM process mechanical properties; however, there is very limited knowledge on such properties of photosensitive resins used in DLP 3D printing and the effect of the printing factors on them. Some researchers, like Stampfl et al. (2008), Liska et al (2007) and Schuster et al. (2007) focus on the chemical composition of the resin to modify the mechanical properties instead of focusing in the printing process itself.

3. Materials and Methodology

The investigation of design-material-process interaction for any process needs a thorough consideration of design aspects of the product being designed, the product raw material, and the manufacturing process needed to produce the part. Given the scope of this paper, the tensile response of a designed part is considered as the main design consideration. For this purpose, a standard design of a tensile specimen is adopted as per ISO 527 (Figure 1b). The primary processing technology is Vat Photopolymerization and the material used is the appropriate photopolymer resin. The following sub-sections provide detailed information on the tools and materials used to carry out this study, as well as the methodology followed and the motivation to start the project.

3.1 Materials and equipment

Printer: the 3D printer used for this study is Ember DLP® by Autodesk. It uses a new 3D printing method in Vat Photopolymerization known as Digital Light Processing (DLP) (Gong et al., 2015). The main difference with classical stereolithography (SL) is that a light projector or Digital Micromirror Device (DMD) is used to define an individual layer at once by the polymerization of the photosensitive resin. A DMD is a semiconductor-based array of light switches. A light source is controlled by the switches using a binary code (Hornbeck, 1997). This results in a simultaneous, dual axis, 2D light projection on the cross-linking or polymerization plane as opposed to a sequential single laser beam scan normally used in SL systems.

Ember has a resolution of 50µm in the plane parallel to the printing surface (XY resolution) and 10µm in the perpendicular plane to the printing surface (Z resolution). The Z resolution is determined by the layer height during the printing process. The printer's build maximum dimensions were reported as 64x40x134mm. The DLP is driven by glass optics and 0.45 WXGA DMD with a 912 x 1140 resolution array manufactured by Texas Instruments.

Software: A solid modelling software was used to design the part; Autodesk Print Studio v1.6.5 was used as a primary computer aided manufacturing software (CAM) for slicing and creating the print files. The primary control firmware for Ember was version 3.0. All data processing was performed using MATLAB R2016a.

Resin Material: PR-48 type of resin was chosen for this study. This resin is also known as Autodesk Standard Clear resin.

Universal Testing Machine: The tensile tests were performed using Bose ElectroForce 3200 Test Instrument.

3.2 Methodology

3.2.1 Pre-processing

Ember's software, Print Studio, provides a total of 64 parameters that can be modified. These parameters are divided into five main groups, namely: support, general, first layer, burn-in layer and model layer. "Support" refers to the extra material that must be added to make sure that the adhesion forces to the building surface are high enough to hold the part in place and to make

sure that every section of the part is connected to said surface at every moment during the printing process.

- Under the "general" section there are three settings to check, namely; anti-alias, grey scale and activation or deactivation of the homing sensor.
- "First layer" parameters are those that refer to the printing settings of the first layer.
- "Burn-in layer" refers to the settings of a number of layers right after the first one, typically less than 10. These layers usually are printed at lower speeds and longer exposure time than the model layers to reaffirm the contact with the building platform.
- "Model layers" are all the layers left after the last burn-in layer.

Due to different layer types during the part fabrication, 16 of the parameters are repeated within the 3 layer groups. On top of the settings offered by the software, other factors such as location, orientation and rotation of the printed parts can be identified, making it a total of 67 factors. From this point of the study, every printer parameter or software setting will be designated as a "factor".

The experiments carried out for this study are a combination of 3 controllable factors out of the 67 identified. These factors were chosen based on the most common controllable factors in DLP printing as a preliminary study to prove the variation in mechanical properties when printing factors are changed. Each factor was assigned 3 levels or values that are summarized in Table 1.

- Factor number 1, layer thickness, represents the total displacement of the Z-axis between each light exposure.
- Factor number 2, exposure time, is the total time that the blue light (405 nm wavelength) is turned on projecting the desired shape over the uncured resin.
- Factor number 3, part orientation presents the alignment of the specimen with the printer's axis.

The physical representation of each orientation level can be observed in Figure 1.

Table 1. Factors and levels

Factor	Level 1	Level 2	Level 3
Layer thickness (μm)	10	25	50
Exposure time	1.6	1.8	2.0
Part orientation	X	Y	Z

The material response was assessed using mechanical tests. The tensile test specimens used were built and tested using Type 1BB specimens of ISO-527-1/2:2012 (ISO527 standard). The specimen type was selected due to the limitation of the maximum load that the testing apparatus can handle during a test. A schematic view of the print patterns and the technical drawing of the specimens can be found in Figure 1. The model was created in SOLIDWORKS®

2015 and then saved as an STL file. The same part was imported 5 times to Print Studio; all the copies were distributed on the printing surface following the same orientation.

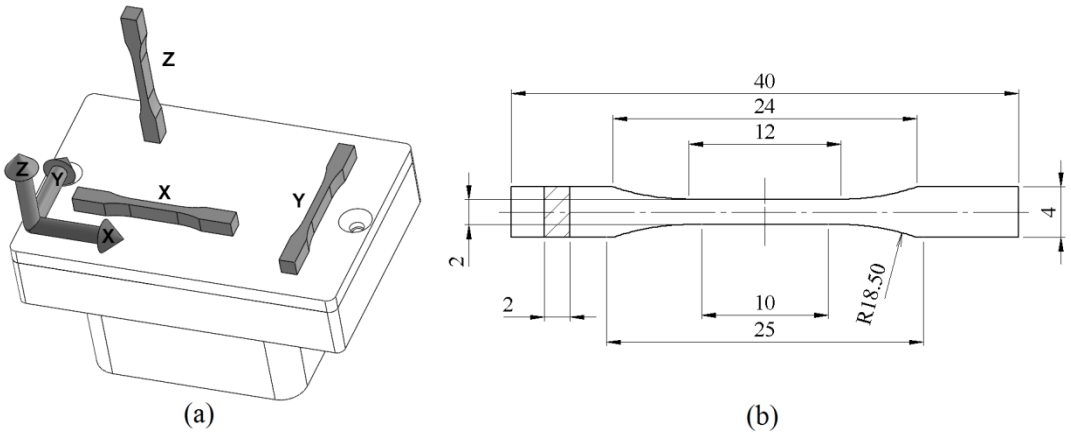

Figure 1. (a) Part orientation levels on the printing surface, and (b) Design of ISO-527-1/2:2012 Type 1BB Test Specimen (ISO, 2012)

Five specimens were prepared for each of the settings mentioned above; resulting in a total of thirty specimens distributed in 6 combinations of levels. Depending on the parameters chosen for each batch, a resulting total print time was obtained. Each print was determined to be representative of one or two print parameters; indicated in bold font in Table 2.

All the specimens were printed in groups of five in order to establish the repeatability of the process; this number was chosen because 5 is the maximum number of specimens that could be fit at the same time on the building surface aligned with the X axis, which was taken as the limiting orientation. It must be noted that the total print time is independent of the number of specimens printed on each batch as long as the orientation is kept constant.

Table 2. Printing factors

Print Number	1	2	3	4	5	6
Print Time	1:29	0:35	0:19	1:51	0:33	0:17
Layer Thickness (μm)	**10**	**25**	**50**	50	25	50
Exposure Time (s)	1.6	1.6	2	**1.6**	**1.8**	**2**
Part Orientation	**Y**	**X**	Y	**Z**	X	X

3.2.2 Post-processing

Directly after the completion of printing process, each part was individually detached from the build surface and immersed in isopropyl alcohol for 3 minutes as recommended by the manufacturer of the machine. Alcohol dissolves any uncured resin and cleans the surface of the parts. Following this, the specimens were left to dry on a clean surface for 24 hours before tested.

The tensile test was performed at a constant speed of 0.01mm/s. The grips were placed at an initial distance of 25 mm from each other. The load cell used for testing the samples was rated

for a maximum force of 400 N. The properties that are investigated were calculated according to the ISO-527:2012 standard (ISO, 2012).

4. Motivation

Based on the previous studies on FDM (Rahman et al., 2015) we can state that a specimen built with layers perpendicular to the direction of the force, as observed in Figure 2, will fail at a lower stress than a specimen printed with layers parallel to the force direction.

Figure 2. Layers result of printing in Z direction

With this study, we aim to find out the best strategies of part placement on the build surface to maximize the ultimate strength. As well, we would like to establish a method to predict the mechanical properties of any part printed with the resin PR-48 with any print setting. To do so, we will analyze the tensile test results of the tested parts, focusing on elastic modulus, ultimate tensile strength and ultimate strain. We will highlight the most significant findings and propose possible justifications.

The total print time will also be analyzed and compared to the tensile test responses. Being time directly related to cost, every finding associated to time can be extended to cost.

Thirty samples were tested at 6 unique combinations of factors. The average elastic modulus, ultimate stress and ultimate strain of the five repetitions for every test are represented in the following section. Each result is grouped and compared among the controllable factors.

5. Results and discussion

In this section, the results of the tensile test will be shown and discussed. The section is divided into three subsections discussing the effect of different factors on: elastic modulus, ultimate stress, ultimate strain and time respectively.

5.1 Tensile Test Results - Elastic modulus

The average elastic modulus of all the specimens tested was 0.749 GPa with a standard deviation of ±0.196 GPa. However, by differentiating the results in terms of the printing factors it can be seen that the moduli follow a trend. This can be observed in Figure 3 where the moduli results are grouped under the four major categories, layer thickness, exposure time, part orientation and printing time.

Elastic modulus vs. **layer thickness**: specimens printed with a layer thickness of 10µm, 25 µm, and 50 µm have an average elastic modulus of 1.031 GPa, 0.719 GPa and 0.651 GPa with a standard deviation of ±0.028 GPa, ±0.046 GPa and ±0.020 GPa, respectively. As can be seen,

increasing layer thickness from 10 µm to 50 µm has decreased the modulus a 37% (from 1.031 to 0.651 GPa). The standard deviation for 25 µm is greater than the others, making the result significantly closer to the 50 µm's than to the 10 µm's. Results also suggest that the smaller the layer, the higher the elastic modulus. This may be due to the exponential decay of light intensity transmission of the resin, getting higher curing rates along the layer and higher adhesion between layers (Jacobs, 1992).

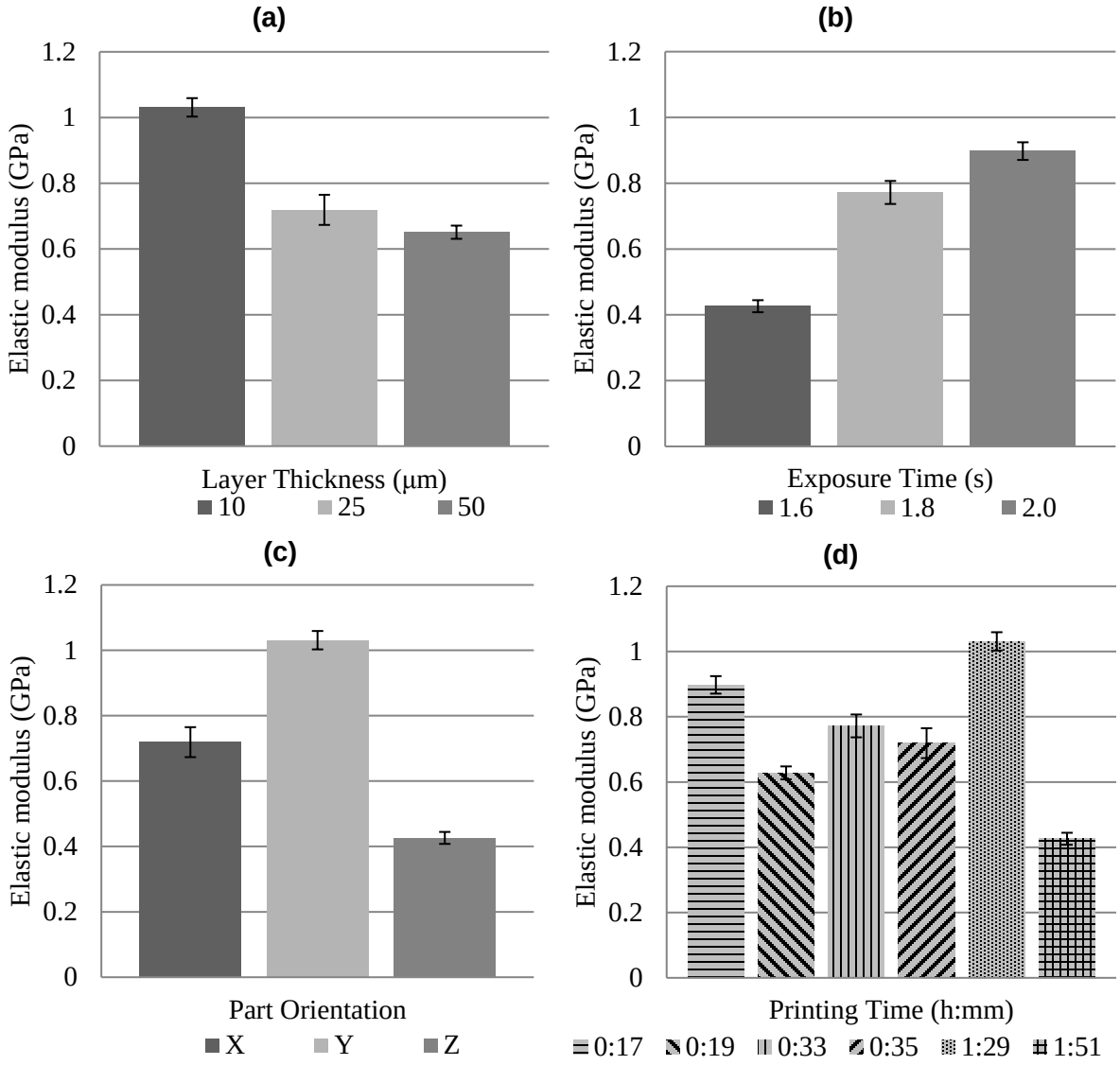

Figure 3. (a) Elastic modulus vs. Layer Thickness, (b) Elastic modulus vs. Exposure time, (c) Elastic modulus vs. Part Orientation, (d) Elastic modulus vs. Printing Time.

Elastic modulus vs. **exposure time**: the inverse trend is observed for the exposure time. Less exposure time implies a lower resulting elastic modulus. This tendency could be associated to the curing of the resin; low curing times implies a less stiff material, while a longer curing time results in a stiffer specimen. In this case, the difference in results is higher between 1.6s (with an average elastic modulus of 0.426 GPa) and 1.8s (with an average elastic modulus of

0.772 GPa) than between 1.8s and 2.0s (with an average elastic modulus of 0.898 GPa). Following the reasons exposed for the layer thickness, a possible explanation for the high elastic modulus for longer exposure times is that more light gets to the previous layer, assuring the adhesion between them.

Elastic modulus vs. **part orientation**: the lowest elastic modulus is observed for the specimen printed in the Z direction, being in average, 0.426 GPa with a low standard deviation of ±0.018 GPa. On the other hand, higher elastic moduli are obtained from the X and Y directions, with an elastic modulus of 0.719 GPa and 1.031 GPa respectively. This result confirms that the lower mechanical properties are those of parts printed along the Z direction. However, X and Y directions should show alike properties due to the printer's configuration.

Elastic modulus vs. **printing time**: the printing time varies between 17 minutes and 1 hour and 51 minutes, as can be observed in Figure 3(d). In this range of time, the average elastic modulus goes from 1031 MPa to 426 MPa. It should be noted that a 25% increase of printing time (1 hour and 29 minutes compared to 1 hour and 51 minutes) leads to a decrease of almost 60% in elastic modulus (1.031 GPa with respect to 0.426 GPa). Finally, as observed in Figure 3(d), where the bars are ordered from short print times to long print times from left to right, long printing times are not directly related to higher elastic modulus.

5.2 Tensile Test Results - Ultimate stress

The average ultimate stress of the 30 tests performed is 21.7 MPa, with a standard deviation of ± 6.5 MPa. The summarized average ultimate stresses can be observed in Figure 4. In a similar way to the elastic modulus, the ultimate stress follows some trends when sorting the results per the factors used.

Ultimate stress vs. **layer thickness**: specimens printed with the thinnest layer thickness can withstand greater forces than those printed with thicker layers, see Figure 4(a). This result can be associated to the resin transmittance, which provides higher degree of curing to a thin layer than to a thicker layer. However, in this case the differences between the 10μm and 25μm can be almost neglected considering the standard deviation of each average ultimate stress, being 26.3 ± 1.4 MPa and 23.0 ± 1.3 MPa. The same effect occurs between 25μm and 50μm, being the average and standard deviation 19.9 ± 0.9 MPa.

Ultimate stress vs. **exposure time**: the results when comparing the exposure times, seen in Figure 4(b), are much more differentiated than the previous ones. Parts whose layers have been cured during 1.6 seconds appear not to be fully cured; hence the average ultimate stress is about three times lower (8.7 MPa) than the stresses under which specimens exposed for 2 seconds break (27.7 MPa).

Ultimate stress vs. **part orientation**: the part orientation plays an important role in the ultimate stress result. Specimens printed along the Z direction show a low ultimate stress. This fact can be related to the adhesion forces between layers oriented perpendicularly to the tensile force direction.

Ultimate stress vs. **printing time**: looking at Figure 4(d) one result must be highlighted; the longest printing time results in an extremely low ultimate stress, only 8.7 MPa; while all the other printing times offer average ultimate stresses between 19.8 MPa and 27.7 MPa. In this case, the longest printing time happens to be parts printed along the Z direction and at 1.6 seconds exposure time; resulting in a brittle piece due to the short exposure time and a long print due to the piece orientation.

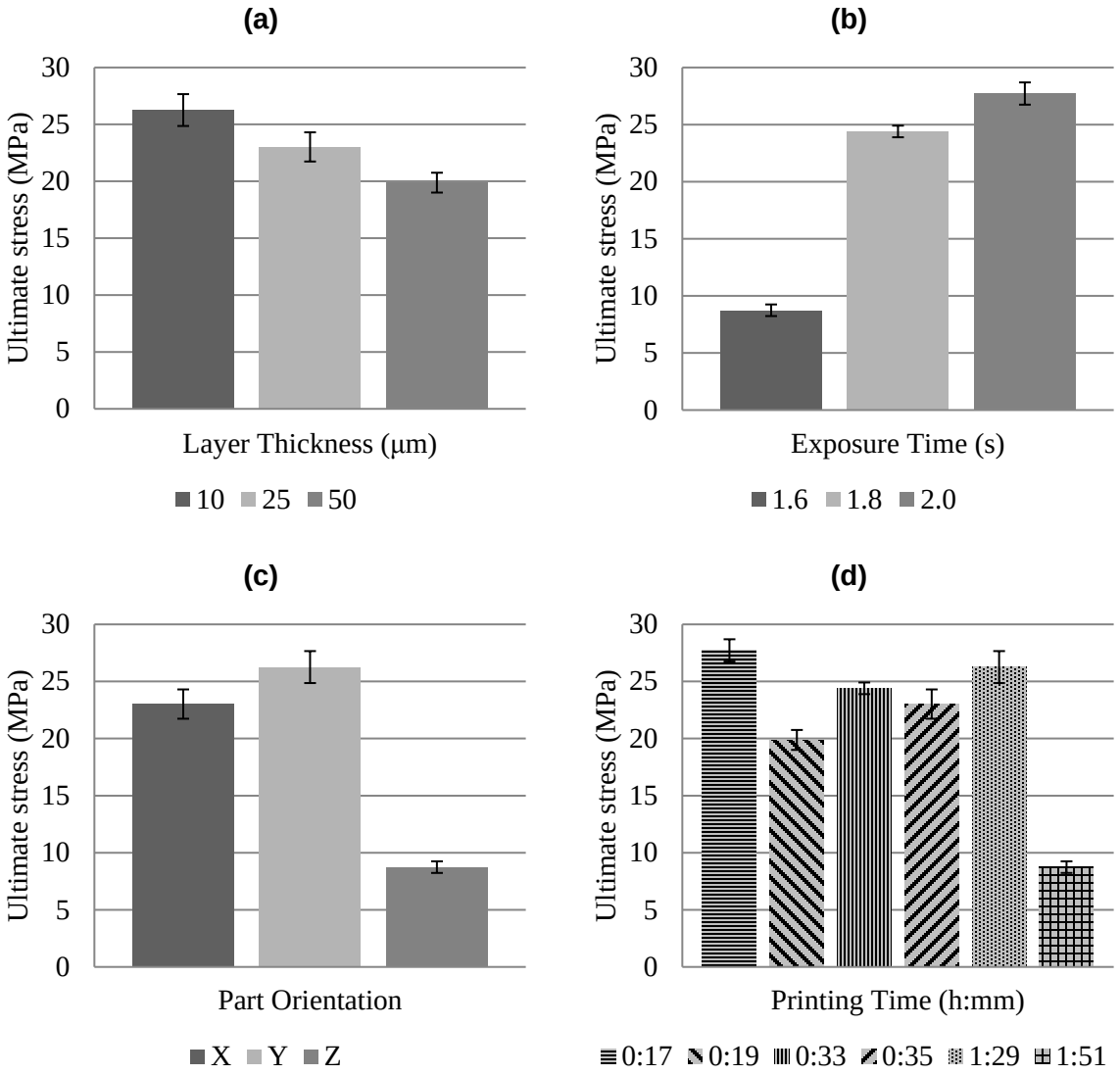

Figure 4. (a) Ultimate stress vs. Layer Thickness, (b) Ultimate stress vs. Exposure time, (c) Ultimate stress vs. Part Orientation, (d) Ultimate stress vs. Printing Time.

5.3 Tensile Test Results - Ultimate strain

The average ultimate strain of all specimens tested was 5.8% a with a standard deviation of ±1.87%. In Figure 5, ultimate strain results are plotted and grouped in terms of the factors analyzed and the total printing time. In general, the results obtained when looking at the ultimate

strain of the specimens, Figure 5, are drastically different than the ones shown previously. In general, the relative standard deviation of the ultimate strain is higher than that of the elastic modulus and ultimate stress.

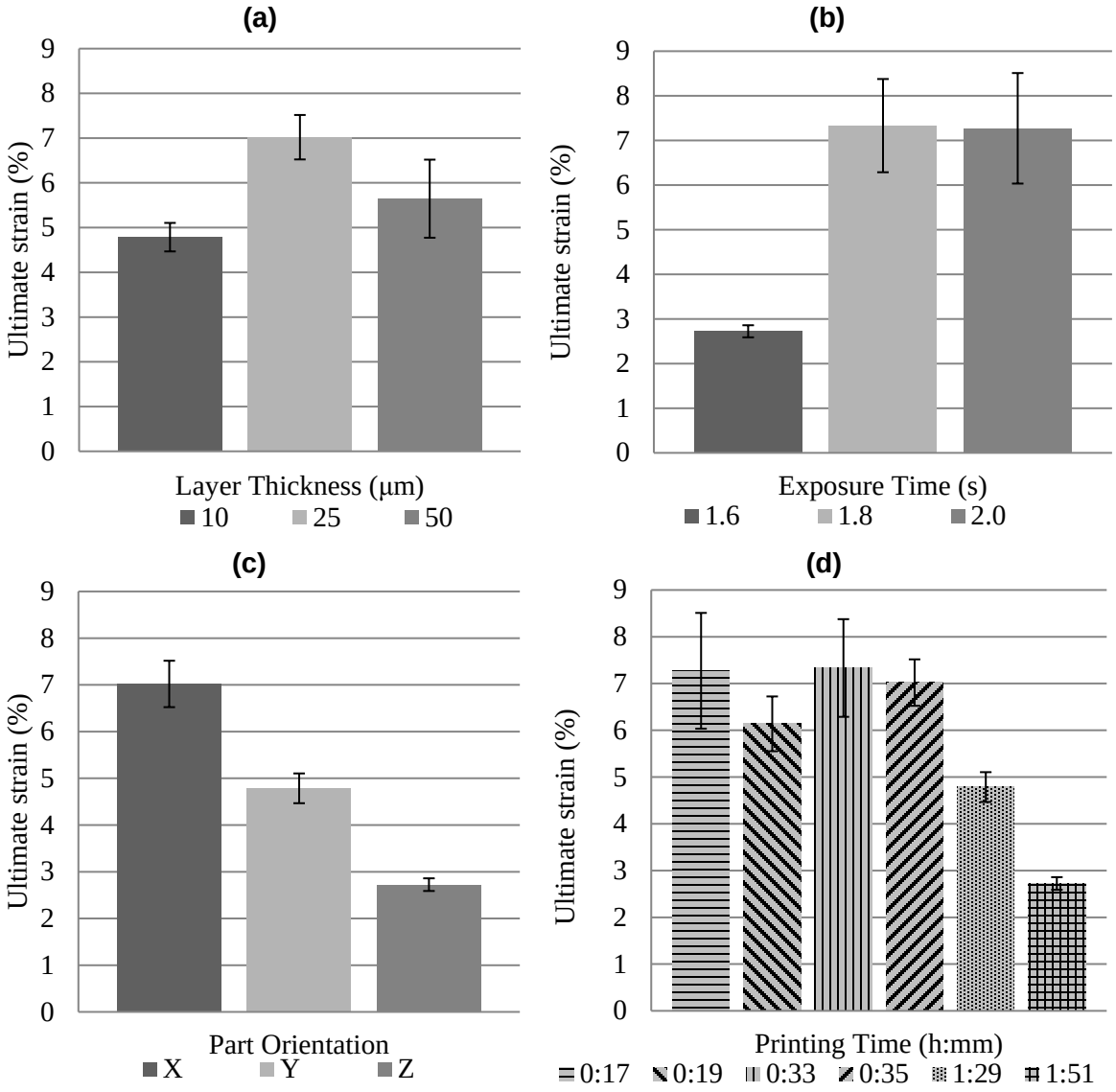

Figure 5. (a) Ultimate strain vs. Layer Thickness, (b) Ultimate strain vs. Exposure Time, (c) Ultimate strain vs. Part Orientation, (d) Ultimate strain vs. Printing Time.

Ultimate strain vs. **layer thickness**: by observing Figure 5(a) the lowest output is obtained with specimens printed with 10μm layers, being the ultimate strain 4.8%; layers of 25μm and 50μm offer ultimate strain results of 7.0% and 5.6% respectively. These last results, when accounting for the standard deviation, overlap with each other; hence, ultimate strains of 25μm and 50μm layers is not so relevant compared to other factors.

Ultimate strain vs. **exposure time**: the exposure time, found in Figure 5(b), brings almost identical ultimate strains for 1.8s and 2.0s (7.33% and 7.27% respectively) suggesting a less

brittle structure than the specimens with only 1.6s of exposure time (ultimate strain of 2.72%). This high difference is due to the higher curing degree of the layers exposed during a longer time; while at 1.6 seconds, the curing degree is lower.

Ultimate strain vs. **part orientation**: parts printed in the Z direction failed at lower strains (2.72%) compared to those printed in the other two directions (7.02% for X and 4.79% for Y). The significant difference between X and Y direction, seen in Figure 5(c) is due to the other factors applied when printing the parts or noise coming from humidity or other sources; given that, theoretically, there should be low to no difference between them.

Ultimate strain vs. **printing time**: there is not a clear relationship between total printing time and ultimate strain, shown in Figure 5(d). The lowest ultimate strain, 2.72%, is the result of the highest printing time, 1hour and 51 minutes. While the one of the highest ones, 7.27%, corresponds to the lowest printing time, 17 minutes. Again, the main reason is that the longest print is for specimens oriented along the Z axis and at low exposure times.

6. Conclusions

Manufacturing processes are an important link of the design-material-process chain and impact the final quality and properties of the part significantly. The considerations or effect of manufacturing process on the product is undertaken during the Design for X (DfX) activities in the product design. In case of traditional/subtractive manufacturing processes, a vast body of design guidelines are available and integrated by product designers in design phase. However, as shown in this paper, there is very limited understanding of the design strategies for Additive Manufacturing processes, specifically for Vat Photopolymerization process. This is complicated by the fact that, unlike the traditional manufacturing processes, the AM processes also exhibit orthotropic behavior; which must be considered while carrying out product design. In order to address this mechanical behavior, the characteristics of the process must be taken into account when carrying out the parametric design of the product.

In this paper, we report on the preliminary findings of ongoing efforts on developing design for additive manufacturing guidelines for Vat Photopolymerization process with a focus on print time, cost, elastic modulus, ultimate tensile stress and ultimate strain. As this paper shows, significant variations between mechanical properties exist for the same designed part printed with different levels of manufacturing process factors. It was shown that variations in the levels of layer thickness, exposure time and part orientation resulted into significant variations in the part quality. A 59% difference in elastic modulus was observed when parameters were changed; this variation was calculated taking the average results. The difference in ultimate stress using different exposure times was 68%. Finally, the maximum strain was proven to change by 63% when the parameters are changed. It was also shown that merely changing the orientation of the part in the printer has a significant effect on the strength of the part.

In addition to the mechanical properties, this paper also sheds light on the economic aspects of the Vat Photopolymerization in terms of time taken to print and its relationship with the mechanical properties. The time needed to print is an important factor representing the machine operating time, hence linked directly to cost of running, depreciation, as well as

maintenance. The paper shows that by varying the factors, the time to print the test sample varies between 17 and 111 minutes, representing an increase of 6.5 times. Moreover, in case of tensile strength the best strength is obtained at the lowest build time.

Considering the results from this study, a more detailed study is being carried out to design and manufacturing parameter optimization for the mechanical properties. This includes an extended design of experiments study to establish the correlation and interaction between different factors. This will result into a comprehensive framework for mechanical properties in function of the printing factors, allowing printing of functional parts; making the DLP printing a viable additive manufacturing process when building specimens that are going to be subjected to external loads.

References

Carroll, B.E., Palmer, T.A. and Beese, A.M. (2015), "Anisotropic tensile behavior of Ti-6Al-4V components fabricated with directed energy deposition additive manufacturing", *Acta Materialia*, Acta Materialia Inc., Vol. 87, pp. 309–320.

Comerford, R. (1993), "A quick look at rapid prototyping", *IEEE Spectrum*, Vol. 30 No. 9, pp. 28–29.

Fatimatuzahraa, A.W., Farahaina, B. and Yusoff, W.A.. (2011), "The effect of employing different raster orientations on the mechanical properties and microstructure of Fused Deposition Modeling parts", *2011 IEEE Symposium on Business, Engineering and Industrial Applications (ISBEIA)*, IEEE, pp. 22–27.

Fuh, J.Y.H., Lu, L., Tan, C.C., Shen, Z.X. and Chew, S. (1999), "Processing and characterising photo-sensitive polymer in the rapid prototyping process", *Journal of Materials Processing Technology*, Vol. 89–90, pp. 211–217.

Gong, H., Beauchamp, M., Perry, S., Woolley, A.T. and Nordin, G.P. (2015), "Optical approach to resin formulation for 3D printed microfluidics", *RSC Adv.*, Royal Society of Chemistry, Vol. 5 No. 129, pp. 3627–3637.

Hornbeck, L.J. (1997), "Digital Light Processing for high-brightness high-resolution applications", in Wu, M.H. (Ed.), *SPIE Projection Displays III*, Vol. 3013, pp. 27–40.

Hull, C.W. (1986), "Apparatus for production of three-dimensional objects by stereolithography", *US Patent 4,575,330*, pp. 1–16.

ISO. (2012), "Plastics - Determination of tensile properties - Part2: Test conditions for moulding and extrusion plastics", *Organization for Standardization*, International Organization for Standardization.

Jacobs, P.F. (1992), *Rapid Prototyping & Manufacturing: Fundamentals of Stereolithography*, Society of Manufacturing Engineers & SME.

Liska, R., Schuster, M., Inführ, R., Turecek, C., Fritscher, C., Seidl, B., Schmidt, V., et al. (2007), "Photopolymers for rapid prototyping", *Journal of Coatings Technology Research*, Vol. 4 No. 4, pp. 505–510.

Mahmood, S., Qureshi, A.J., Goh, K.L. and Talamona, D. (2017), "Tensile strength of partially filled FFF printed parts: experimental results", *Rapid Prototyping Journal*, Vol. 23 No. 1, pp. 122–128.

Qureshi, A.., Mahmood, S., Wong, W.L.. and Talamona, D. (2015), "Design for Scalability and Strength Optimisation for components created through FDM process", *Iced 2015*, pp. 1–12.

Rahman, K.M., Letcher, T. and Reese, R. (2015), "Mechanical Properties of Additively Manufactured PEEK Components Using Fused Filament Fabrication", *Volume 2A: Advanced Manufacturing*, ASME, p. V02AT02A009.

Salmoria, G.V., Ahrens, C.H., Fredel, M., Soldi, V. and Pires, A.T.N. (2005), "Stereolithography somos 7110 resin: mechanical behavior and fractography of parts post-cured by different methods", *Polymer Testing*, Vol. 24 No. 2, pp. 157–162.

Santos, A.R.C., Almeida, H. a. and Bártolo, P.J. (2013), "Additive manufacturing techniques for scaffold-based cartilage tissue engineering", *Virtual and Physical Prototyping*, Taylor & Francis, Vol. 8 No. 3, pp. 175–186.

Schuster, M., Turecek, C., Kaiser, B., Stampfl, J., Liska, R. and Varga, F. (2007), "Evaluation of Biocompatible Photopolymers I: Photoreactivity and Mechanical Properties of Reactive Diluents", *Journal of Macromolecular Science, Part A*, Vol. 44 No. 5, pp. 547–557.

Stampfl, J., Baudis, S., Heller, C., Liska, R., Neumeister, a, Kling, R., Ostendorf, a, et al. (2008), "Photopolymers with tunable mechanical properties processed by laser-based high-resolution stereolithography", *Journal of Micromechanics and Microengineering*, Vol. 18 No. 12, p. 125014.

Wong, K. V and Hernandez, A. (2012), "A Review of Additive Manufacturing", *ISRN Mechanical Engineering*, Vol. 2012, pp. 1–10.

Acknowledgments

The authors would like to acknowledge the funds provided by Natural Sciences and Engineering Research Council of Canada (NSERC) - Discovery Grants (418533 and RGPIN-2016-04689) and the University of Alberta Mechanical Engineering Department that allowed this research to be conducted. The authors also would like to acknowledge the funds provided by Canadian Foundation for Innovation (CFI - Project #31500).